

Electrochemical Characterization of Nanosized Electrode Arrays Prepared from Nanoporous Self-Assembled Monolayers

Shin-Jung Choi and Su-Moon Park*

Department of Chemistry and Center for Integrated Molecular Systems,
Pohang University of Science and Technology, Pohang, Kyungbuk 790-784, Korea
Received January 14, 2002

We characterized nanoelectrode arrays prepared from self-assembled monolayers (SAMs) by adsorption from a solution containing thiolated β -cyclodextrin (β -CD) and *n*-alkanethiol on the gold electrode surface, using electrochemical methods. While the framework, the *n*-hexadecanethiol SAM, effectively blocked electron transfer between the electrode surface and solution-phase redox probe molecules, the β -CD cavities isolated in the forests of *n*-hexadecanethiol molecules were shown to act as an ultramicroelectrode array. The shapes of cyclic voltammograms of probe molecules were related to the number densities of β -CD molecules within the monolayer films. Probe molecules that have the correct combination of physical and chemical characteristics were shown to effectively penetrate the framework through the β -CD pores and exchange electrons with the electrode surface.

Keywords : Nanoporous, Nanoelectrode arrays, Thiolated β -cyclodextrin, Self-assembled monolayers, Molecular selectivity.

Introduction

Ultramicroelectrodes (UMEs) have seen increased applications due to their capability of producing the dramatically improved signal-to-noise ratios for voltammetric data.¹ Depending on the experimental conditions, the capability includes the increased temporal resolution, the increased current density, and the decreased sensitivity to the effects of solution resistance. In addition, previously impossible experiments have been made possible with UMEs. The electrochemical responses at UMEs differ greatly from those seen at electrodes of conventional size. When operated on the time scale of seconds, the dimensions of the UMEs are smaller than the diffusion layer thickness of the redox active molecules in solution. As a result, the flux becomes very large at UMEs leading to a steady-state response.

In this study, we used self-assembled monolayers (SAMs) prepared using a mixed solution of thiolated β -cyclodextrin and *n*-alkanethiol with an appropriate ratio on the gold electrode surface in order to prepare nanoelectrode arrays. Crooks *et al.*² introduced a similar concept by preparing mixed SAMs on gold electrodes using solutions containing appropriate ratios of *n*-alkanethiols and 4-aminothiophenol (4-ATP). Islands of electroactive 4-ATP aggregates formed among electrochemically inert *n*-alkanethiol SAMs acted as a microelectrode array. This concept was later refined using thiolated β -CD molecules,³ which have better defined cavity sizes compared to the 4-ATP aggregates formed as a result of a thermodynamic compromise between the 4-ATP and *n*-alkanethiol molecules.

We found that the thiolated β -CD molecules make an

almost ideal SAM when the unoccupied space between β -CD molecules is sealed with *n*-hexadecanethiol molecules that also adsorb strongly on the gold surface.³⁻⁵ Recently, we have demonstrated that the β -CD cavities can be separated from each other by controlling molar ratios of thiolated β -CD and *n*-hexadecanethiol, which forms a rather strong SAM of its own between β -CD molecules on the surface.⁴ Each β -CD cavity can be isolated in thick forests of *n*-hexadecanethiol and, therefore, can act as a nanoelectrode array. When thiolated α - and β -CD molecules form SAMs on gold electrodes, they showed molecular size selectivity for electroactive compounds such as *p*-benzoquinone (BQ), 2-methylnaphthaquinone, and anthraquinone, which have different molecular sizes.³ The CD-SAMs thus prepared were also used as templates for the preparation of nanodots of semiconductor materials and nanowires of conducting polymers.^{4,5}

In this report, we describe results obtained from various voltammetric experiments to characterize the SAM-modified electrodes having β -CD pores among the *n*-hexadecanethiol forests as an UME array. To achieve our primary goal of understanding the behavior of the nanoelectrode arrays thus prepared at the molecular level, it is important to address the following three questions: (1) how stable the β -CD-induced active sites are; (2) whether or not these structures can be visualized directly or indirectly and if so, what is the geometrical relationship between the template molecules, β -CD, and the framework molecules, *n*-hexadecanethiol; and (3) in what form redox probe molecules would enter the pores. Now we begin to address these three questions.

Experimental Section

Reagent grade β -CD (Aldrich), dimethylsulfoxide (DMSO,

*Corresponding Author. E-mail: smpark@postech.edu; Fax: +82-54-279-3399

Aldrich), *n*-pentanethiol (Aldrich), *n*-decanethiol (Aldrich), *n*-hexadecanethiol (Aldrich), ferrocene (FeCp_2 , Aldrich), ethanol (EtOH, J. T. Baker), $\text{Ru}(\text{NH}_3)_6\text{Cl}_3$ (Aldrich), $\text{K}_3\text{Fe}(\text{CN})_6$ (Aldrich), *p*-benzoquinone (BQ, Adrich), KCl (Aldrich), KNO_3 (Aldrich), H_2SO_4 (Shinyo Pure Chemical), and H_2O_2 (Junsei Chemical) were used as received. Doubly distilled water was used for the preparation of solutions. Thiolated β -CD was prepared according to the procedure previously reported.⁶

For electrochemical experiments, we used a gold disk electrode with an area of 0.022 cm^2 , which was cleaned in a piranha solution ($\text{H}_2\text{SO}_4 : \text{H}_2\text{O}_2 = 70 : 30$), and rinsed with doubly distilled, deionized water before each experiment. The SAMs were prepared by dipping the gold electrode in a solution containing an appropriate ratio of thiolated β -CD, *n*-hexadecanethiol, and FeCp_2 in a mixed solvent (DMSO : EtOH : $\text{H}_2\text{O} = 5 : 3 : 2$). These three compounds have different polarities leading to different solubility in a fixed solvent, and a mixture of three solvents was found satisfactory for preparation of the SAMs. Cyclodextrins and hexadecanethiols are soluble in DMSO and ethyl alcohol, respectively. The FeCp_2 molecules were used to protect β -CD cavities during this process; FeCp_2 forms inclusion complexes inside the β -CD cavities, which prevent the cavities from being occupied by *n*-alkanethiol molecules.^{3,6} The *n*-alkanethiol molecules are only to form a uniform, defectless SAM on the gold surface between well separated β -CD cavities. The modification of the gold electrode with the SAM was achieved by immersing the gold electrode in the above solution for different lengths of time depending on experiments, and then washing the electrode surface with EtOH and doubly distilled, deionized water to remove unadsorbed thiolated β -CD, *n*-alkanethiol, and FeCp_2 captured inside the cavities.

An EG&G Princeton Applied Research model 273A potentiostat-galvanostat was used to record cyclic voltammograms. A three electrode cell were employed for electrochemical experiments. Gold disk, Pt wire or foil, and $\text{Ag}|\text{AgCl}$ (in saturated KCl) electrodes were used as working, counter, and reference electrodes, respectively.

Results and Discussion

Electrochemical techniques based on cyclic voltammetry have been used for analyzing the integrity of the SAMs and their structures. These include measurements of the electron transfer rate using electroactive probe molecules, capacitance measurements, and oxidation of exposed gold surfaces.² In this work, we describe electrochemical characterization of *n*-alkanethiol monolayers of different chain lengths on gold electrodes.

We examined the nature and extent of the structural defects of the *n*-alkanethiol SAMs by electrochemical measurements. In these experiments, $\text{Fe}(\text{CN})_6^{3-}$ was used as a redox probe molecule. Figure 1 shows CVs recorded for $\text{Fe}(\text{CN})_6^{3-}$ reduction at the gold electrode as a function of exposure time to the solutions containing *n*-alkanethiol of various chain

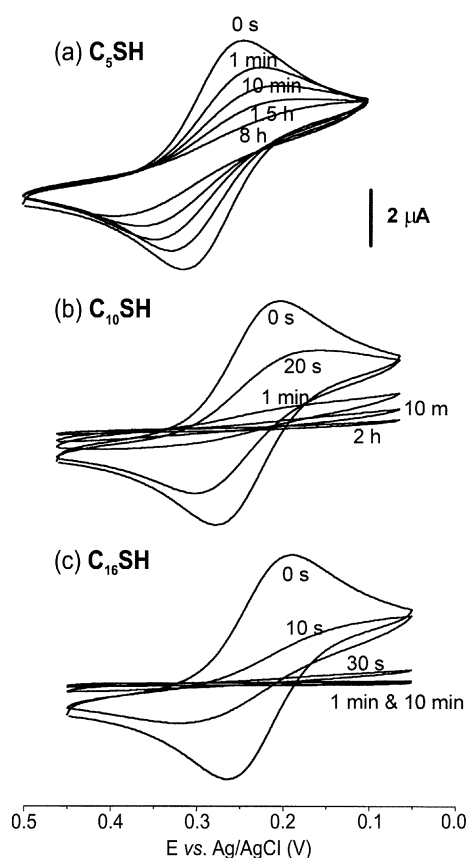


Figure 1. CVs recorded as a function of their exposure time at a gold electrode in aqueous solution containing $1.0 \text{ mM K}_3\text{Fe}(\text{CN})_6$ and 0.10 M KNO_3 at 50 mV/s . The electrode was prepared by exposing it for the exposure time indicated on the CVs in a DMSO-ethanol-water mixed solution containing 1.0 mM solution of (a) *n*- $\text{C}_5\text{H}_{11}\text{SH}$, (b) *n*- $\text{C}_{10}\text{H}_{21}\text{SH}$, or (c) *n*- $\text{C}_{16}\text{H}_{31}\text{SH}$.

lengths. As can be seen, SAMs of long-chain *n*-alkanethiol molecules are free of measurable pin-holes and provided substantial resistance to electron transfer (Figure 1c). In contrast, short-chain monolayers provided a weak barrier to ion penetration indicating that a number of defects are present in the SAM structure (Figure 1a). This is attributed to different free energies of gold-sulfur bond formation depending on the chain length of alkylthiols due to the difference in van der Waals energy between alkyl chains. Nuzzo *et al.*⁷ reported the stabilization energy of $0.8 \text{ kcal}/(\text{mol CH}_2)$ for the formation of alkylthiol SAMs on gold surfaces. As a result, the short chain alkylthiols have a smaller free energy of bond formation and, thus, are undergoing constant exchange reactions between molecules adsorbed on the surface and those in solution.

The *n*-hexadecanethiol molecules act as an electron- and mass-transfer blocking layer, while the β -CD molecules act as electron-transfer sites, introducing openings among the alkanethiol SAMs. Figure 2 shows CVs recorded in a $\text{Ru}(\text{NH}_3)_6\text{Cl}_3$ solution. The $\text{Ru}(\text{NH}_3)_6^{3+}$, which is capable of exchanging electrons with the electrode surface through the gate sites, was used as a probe molecule to characterize the nanoporous monolayer films. Here, a gold electrode was

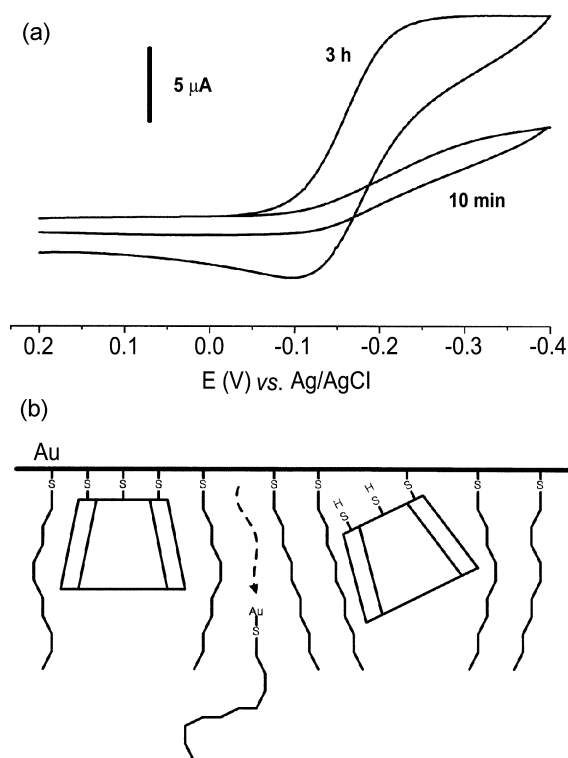


Figure 2. (a) CVs recorded for the 5 mM $\text{Ru}(\text{NH}_3)_6\text{Cl}_3$ and 0.5 M KCl solution at 100 mV/s at a gold electrode as a function of exposure time to a mixed solution of 1.0 mM thiolated β -CD and 1.0 mM *n*-hexadecanethiol in the mixed solvent and (b) a schematic view of a dynamic and reversible adsorption process. Again, the electrode was prepared by exposing it to the above mixed solution for the designated period.

immersed in a solution containing a molar ratio of β -CD to *n*-hexadecanethiol of 1 for 10 min and 3 h. As time goes on, the limiting currents were seen to be changed. It means that the adsorption process is dynamic and reversible. The dynamic and reversible adsorption process is part of the mechanism for attaining equilibrium adsorption coverage by maximizing the packing density.^{2,8-10} The dynamic nature of the equilibrium has been demonstrated by exchange reactions such as the exchange of *n*-alkanethiols with ferrocene-labeled alkanethiols⁸ and self-exchange of isotopically labeled compounds.¹⁰

The voltammograms shown in Figure 2a reveal a trend towards an increasing faradaic current for $\text{Ru}(\text{NH}_3)_6\text{Cl}_3$ reduction over time through β -CD-induced pores in the SAM. Since the SAM formed for 10 minutes in a pure *n*-hexadecanethiol solution yields a largely passive electrode for electron transfer (see Figure 1c), we believe that the initial contact of the gold surface with the β -CD/*n*-hexadecanethiol mixed solution results in a high surface concentration of *n*-hexadecanethiol, which is being replaced slowly by thiolated β -CD as time goes on.

While the *n*-hexadecanethiol SAM having only one -SH group in one molecule shows a dynamic and reversible adsorption process, the adsorption process of thiolated β -CD does not appear so dynamic. Ideally, a thiolated β -CD

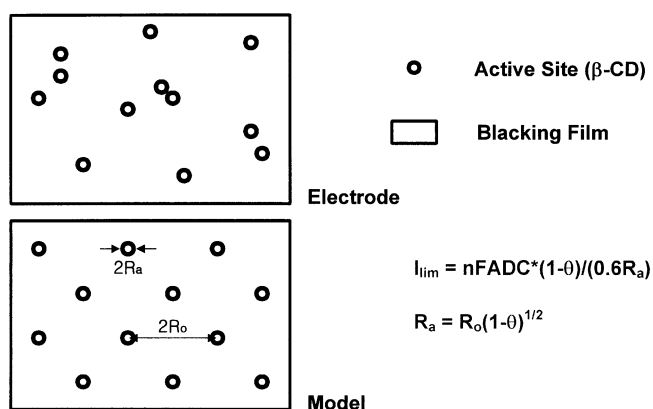


Figure 3. A model proposed for an ultramicroelectrode array by Amatore and co-workers.¹⁰

molecule contains seven -SH groups, and once one Au-S bond is formed, it would be easier for the other six -SH groups to bind with the gold surface due to their proximity to the gold surface. In addition, it would be difficult for the β -CD bonded to gold to be detached because the multiple Au-S bonds must be broken simultaneously to detach the β -CD from the gold surface (Figure 2b).

We have performed a semi-quantitative analysis of the data using a theoretical model developed by Amatore *et al.*¹¹ Amatore *et al.* proposed a theory for obtaining quantitative data for UME arrays¹¹ (Figure 3). They showed that the results of cyclic voltammetric experiments permit a quantitative evaluation of the average size and spatial distribution of the active sites. They also derived a relation for the average size and the average distance between active sites in a blocking film. According to their model, the limiting plateau current, i_{lim} , of the steady-state cyclic voltammogram (CV) is related to the fractional surface coverage, Θ , and the average distance between the centers of two adjacent active sites, $2R_o$, as given by Eq. (1).

$$i_{\text{lim}} = nFADC^*(1-\Theta)^{1/2}/(0.6R_o) \quad (1)$$

Here, F is the Faraday constant, A is the geometrically projected surface area of the electrode, D is the diffusion coefficient of the electroactive species, C^* is its bulk concentration of the probe molecule, and Θ is the fractional coverage of the electrode by the blocking film. The relationship between the average active site radius, R_a , and distance between the active sites, $2R_o$, is given by Eq. (2).

$$R_a = R_o(1-\Theta)^{1/2} \quad (2)$$

Combination of Eq. (1) and Eq. (2) results in an expression for i_{lim} as a function of both the active site radius, R_a , and the fractional surface coverage of the active sites, $(1-\Theta)$:

$$i_{\text{lim}} = nFADC^*(1-\Theta)/(0.6R_a). \quad (3)$$

Eq. (3) is used to calculate the theoretical limiting current that results from radial diffusion. To obtain reliable results using this model, the average distance between defects, $2R_o$, must be greater than the diffusion layer during the time scale

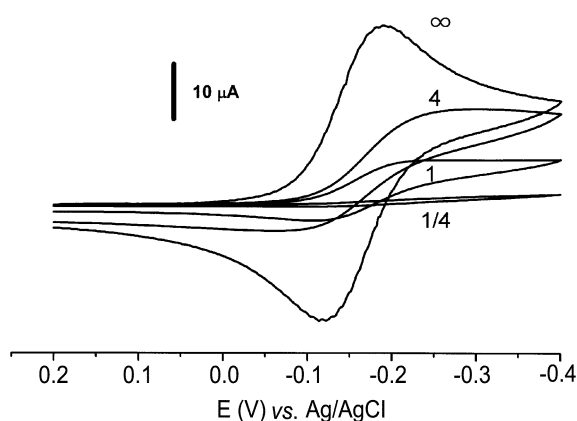


Figure 4. CVs obtained from a solution of 5 mM $\text{Ru}(\text{NH}_3)_6\text{Cl}_3$ and 0.5 M KCl at the mixed SAM-modified electrode prepared by soaking it in the solutions of various ratios of β -CD: n -hexadecanethiol. The molar ratios of β -CD to n -hexadecanethiol were ∞ , 4, 1, and 1/4 and the scan rate was 100 mV/s in all cases.

of the experiment. That is, the individual diffusion layers should not overlap with each other.

To directly correlate the calculated and experimental values of the limiting current, we must know both the size and the number density of the active sites. With an R_a value of 0.80 nm¹² (the inner diameter of β -CD), we can calculate the Θ value from the experimental limiting current. From the CV recorded at the SAM-modified electrode prepared by immersing the gold electrode in the (1 : 1) mixed thiol solution for 3 hours, Eq. (2) yields $1-\Theta$ value of 4.4×10^{-6} . To put it differently, this means that the average distance between the β -CD cavities, $2R_o$, is about 400 nm and there are about $10^9/\text{cm}^2$ of β -CD-induced pores on the electrode surface.

The CVs shown in Figure 4 were obtained from the electrode prepared by soaking it in the solutions containing various ratios of β -CD and n -hexadecanethiol. The SAMs used for this experiment and experiments for Figures 5 and 6 were prepared by immersing the electrode in a mixed solution containing β -CD and n -hexadecanethiol for three hours as reproducible results were obtained when the SAMs were obtained by immersing the electrode at least three hours. The CV for the $\text{Ru}(\text{NH}_3)_6^{3+/2+}$ pair at the gold electrode coated only with β -CD (the β -CD to n -hexadecanethiol ratio is ∞) is almost the same as that at the bare gold electrode. That is, the CV expected from the linear diffusion was obtained, which agrees with our previous results.³ When β -CD is incorporated into the n -hexadecanethiol monolayer, the CV shapes resemble that from radial diffusion. A few points are noteworthy in the CVs shown in Figure 4. First, the current decreases as the relative fraction of β -CD decreases on the surface indicating that the β -CD pores permit $\text{Ru}(\text{NH}_3)_6^{3+}$ to reach the electrode surface. When there is no β -CD cavity, no currents flow after 10 min of exposure of the gold surface to the solution containing only n -hexadecanethiol as was seen from Figure 1c. Second, as the ratio of β -CD to n -hexadecanethiol is decreased in the solution, the limiting current also decreases and becomes more sigmoidal, suggesting that the intercavity distance

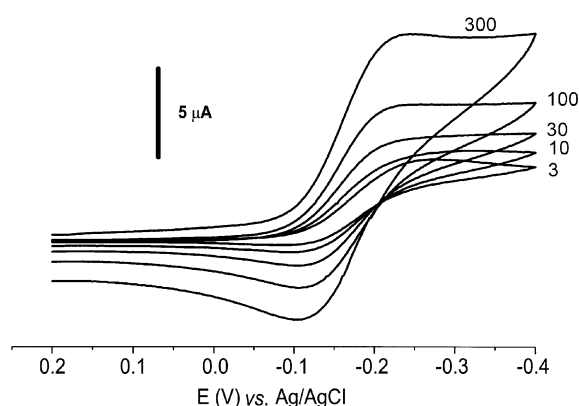


Figure 5. CVs recorded at the mixed SAM-covered gold electrode as a function of scan rate. The scan rates were 3, 10, 30, 100, and 300 mV/s. The solution contained 5 mM $\text{Ru}(\text{NH}_3)_6\text{Cl}_3$ and 0.5 M KCl. The SAMs on gold were formed from a mixed solution of 1.0 mM β -CD and 1.0 mM n -hexadecanethiol.

becomes larger compared to the diffusion layer thickness. As a result, the linear diffusion, which is observed at the electrode prepared from the solution of the high β -CD to n -hexadecanethiol ratio, changes to the radial diffusion when it is modified in a solution containing the low concentration ratio of β -CD to n -hexadecanethiol. Third, the n -hexadecanethiol molecules in the solution compete more effectively for surface adsorption than β -CD molecules as can be seen from the current shown in Figure 4, which becomes sigmoidal even at the fairly high concentration ratio of β -CD to n -hexadecanethiol in solution.

Figure 5 shows the scan rate dependency for the redox reaction of a $\text{Ru}(\text{NH}_3)_6^{3+}$ solution at the nanoporous SAM-modified gold electrode prepared from the mixed solution of (1 : 1) β -CD and n -hexadecanethiol for 3 hours. There are two important points to note here. First, the voltammograms are well behaved between the scan rate of 3 to 300 mV/s with the change in current of less than 2.5 times. For the pure radial diffusion behavior, we would predict no change in current, while the pure linear diffusion would yield an increase of 10 times.¹³ This suggests that the current is controlled primarily by the radial diffusion. Second, the shape of the voltammograms becomes more characteristic of linear diffusion at faster scan rates as is evidenced from the forward and reverse peak currents. This observation serves to confirm our assertion that nanoporous SAMs are characterized as an array of very small UMEs; the linear diffusion component is obtained due to the linear diffusion component at a shorter electrolysis time or a faster scan rates.^{13a} In general, the contribution from the spherical diffusion becomes smaller at higher scan rates, leading to a deviation from the ideal radial diffusion behavior.^{13b}

Figure 6 shows a series of voltammograms obtained at bare and SAM modified electrodes in the presence of the three different probe molecules: $\text{Ru}(\text{NH}_3)_6^{3+}$, $\text{Fe}(\text{CN})_6^{3-}$, and benzoquinone (BQ). Although the concentrations of the three probe molecules are the same, the peak current of BQ is twice of those for $\text{Ru}(\text{NH}_3)_6^{3+}$ and $\text{Fe}(\text{CN})_6^{3-}$ as shown in

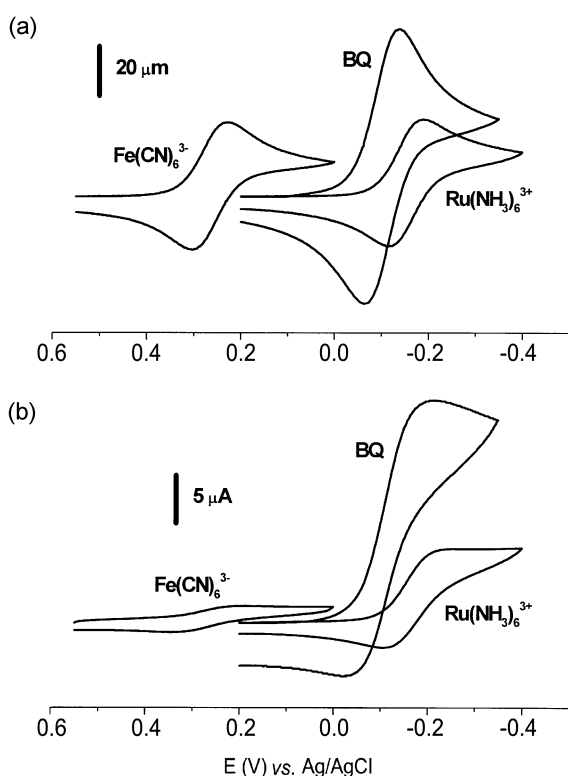


Figure 6. CVs obtained at (a) bare and (b) mixed SAM-covered gold electrodes in the presence of 5 mM of the three different probe molecules: $\text{Ru}(\text{NH}_3)_6^{3+}$, BQ, and $\text{Fe}(\text{CN})_6^{3-}$. The scan rate was 100 mV/s in all cases. The SAM on gold was formed from a mixed solution of 1.0 mM β -CD and 1.0 mM *n*-hexadecanethiol.

Figure 6a where voltammograms were recorded at the bare gold electrode. The redox reaction between BQ and hydroquinone is two-electron transfer reaction. However, the limiting current for $\text{Fe}(\text{CN})_6^{3-}$ reduction is significantly smaller than those for $\text{Ru}(\text{NH}_3)_6^{3+}$ and BQ in voltammograms recorded at the mixed SAM modified electrode (Figure 6b). This is attributed to the larger permeability of the pores to $\text{Ru}(\text{NH}_3)_6^{3+}$ and BQ than to $\text{Fe}(\text{CN})_6^{3-}$. Although the total number and average size of the pores are fixed, there are differences in the nature of the intermolecular interaction between the probe molecules and the pores. This important observation indicates that the pores show selectivity for the probe molecules based on their chemical nature.

Table 1 summarizes the structures and properties of probe molecules. As shown in Figure 6b, the limiting current of $\text{Ru}(\text{NH}_3)_6^{3+}$ is much larger than that of $\text{Fe}(\text{CN})_6^{3-}$. The ionic charge of the cavity should contribute to the discrimination of $\text{Ru}(\text{NH}_3)_6^{3+}$ against $\text{Fe}(\text{CN})_6^{3-}$. Since the inside of the β -CD cavity would be somewhat negatively charged with a number of oxygen atoms, positively charged molecules would penetrate more effectively than negatively charged ones.

The sigmoidal shape of the voltammogram shown for $\text{Ru}(\text{NH}_3)_6^{3+}$ is characteristic of the radial diffusion to the pore sites. However, the voltammogram observed for BQ must have both the linear and radial diffusion components

Table 1. An illustration of the structures and properties of probe molecules^a

	Diameter	6.4 Å
	D	$7.1 \times 10^{-6} \text{ cm}^2/\text{s}$
	k°	$> 1 \text{ cm/s}$
	diameter	6.0 Å
	D	$8.3 \times 10^{-6} \text{ cm}^2/\text{s}$
	k°	0.15 cm/s
	Height	5.4 Å
	width	4.3 Å
	D	$8 \times 10^{-6} \text{ cm}^2/\text{s}$
	k°	$1 \times 10^{-3} \text{ cm/s}$

^aTaken from Ref. 2a.

due to overlapping diffusion layers. Since the electrodes used to obtain the two CVs were exactly the same, we conclude that some pore sites accessible to BQ may not be accessible to $\text{Ru}(\text{NH}_3)_6^{3+}$. Further, the difference in diffusion coefficients of these two electroactive compounds might have caused the differences in voltammetric shapes of these compounds. It is certain that there is a degree of molecular recognition based on some properties of the probe molecules.

In general, the β -CD cavities favor nonpolar compounds, and they form complexes with them.¹⁴ Host-guest interactions through these cavities lead to the formation of inclusion complexes with guest molecules. Driving forces for the formation of the β -CD inclusion complex arise from apolar/apolar interactions between guest molecules and host cavities, the β -CD-ring strain release on complexation, and van der Waals interactions. It seems that the discrimination of the β -CD cavity against ferricyanide is based on electric field effects for the charged molecules as well as chemical and physical interactions between the cavities and probe molecules.

Conclusions

We characterized nanoporous films using electrochemical methods. The framework, *n*-hexadecanethiol, of the monolayer was sufficiently thick that it effectively blocked electron transfer between the electrode surface and solution-phase redox probe molecules. The shape of the resulting CV could be related to the size and number density of pores within the film. As the ratio of β -CD to *n*-hexadecanethiol in the deposition solution was increased, the limiting current also increases and an increased departure from the voltammetric behavior expected from radial diffusion was observed. However, probe molecules with the correct combination of physical and chemical characteristics could penetrate the framework through β -CD-induced pore sites and exchange electrons with the Au electrode surface. Our key finding is

that only molecules with the correct combination of intermolecular interactions, hydrated radius and ionic charges could penetrate the framework. Our results suggest that UMEs having chemical selectivities can be designed successfully by employing appropriate molecules for the formation of SAMs on gold electrodes. Work is in progress along this line in our laboratory.

Acknowledgment. This work was supported by a grant from the Korea Research Foundation (KRF-2001-DS0035) and BK21 program of the same foundation.

References

1. Wightman, R. M.; Wipf, D. O. "Voltammetry at Ultramicroelectrodes" in *Electroanalytical Chemistry*, Vol. 15; Bard, A. J., Ed.; Dekker: New York, 1989; pp 267-353.
2. (a) Chailapakul, O.; Crooks, R. M. *Langmuir* **1993**, *9*, 884. (b) Chailapakul, O.; Crooks, R. M. *Langmuir* **1995**, *11*, 1329, and references therein.
3. Lee, J.-Y.; Park, S.-M. *J. Phys. Chem. B* **1998**, *102*, 9940.
4. Lee, J.-Y.; Park, S.-M. *J. Electrochem. Soc.* **2000**, *147*, 4189.
5. (a) Choi, S.-J.; Woo, D.-H.; Myung, N.; Kang, H.; Park, S.-M. *J. Electrochem. Soc.* **2001**, *148*, C569; (b) Woo, D.-H.; Choi, S.-J.; Han, D.-H.; Kang, H.; Park, S.-M. *Phys. Chem. Chem. Phys.* **2001**, *3*, 3382; (c) Choi, S.-J.; Park, S.-M. *Adv. Mater.* **2000**, *12*, 1547; (d) Park, S.-M.; Lee, J.-Y.; Choi, S.-J. *Synth. Met.* **2001**, *121*, 1297.
6. (a) Rojas, M. T.; Königer, R.; Stoddart, J. F.; Kaifer, A. E. *J. Am. Chem. Soc.* **1995**, *117*, 336; (b) Gadelle, A.; Defaye, J. *Angew. Chem. Int. Ed. Engl.* **1991**, *30*, 78.
7. (a) Nuzzo, R. G.; Dubois, L. H.; Allara, D. L. *J. Am. Chem. Soc.* **1990**, *112*, 558; (b) Dubois, L. H. *Annu. Rev. Phys. Chem.* **1992**, *43*, 437.
8. Hahner, G.; Woll, Ch.; Buck, M.; Grunze, M. *Langmuir* **1993**, *9*, 1955.
9. Chidsey, C. D. E.; Bertozzi, C. R.; Putvinski, T. M.; Mujisce, A. M. *J. Am. Chem. Soc.* **1990**, *112*, 4301.
10. Collard, D. M.; Fox, M. A. *Langmuir* **1991**, *7*, 1192.
11. Amatore, C.; Saveant, J. M.; Tessier, D. *J. Electroanal. Chem.* **1983**, *147*, 39.
12. Li, S.; Purdy, W. C. *Chem. Rev.* **1992**, *92*, 1457.
13. Bard, A. J.; Faulkner, L. R. *Electrochemical Methods*, 2nd Ed.; Wiley: New York, 2001, (a) p 168; and (b) p 232.
14. (a) Inoue, Y.; Hakushi, T.; Liu, Y.; Tong, L.-H.; Shen, B.-J.; Jin, D.-S. *J. Am. Chem. Soc.* **1993**, *115*, 475; (b) Hamasaki, K.; Ikeda, H.; Nakamura, A.; Ueno, A.; Toda, F.; Suzuki, I.; Osa, T. *J. Am. Chem. Soc.* **1993**, *115*, 5035; (c) Breslow, R.; Zhang, B. *J. Am. Chem. Soc.* **1996**, *118*, 8495; (d) Isnin, R.; Salam, C.; Kaifer, A. E. *J. Org. Chem.* **1991**, *56*, 35; (e) Godinez, L. A.; Lin, J.; Munoz, M.; Coleman, A. W.; Kaifer, A. E. *J. Chem. Soc., Faraday Trans.* **1996**, *92*, 645; (f) Wenz, G. *Angew. Chem. Int. Ed. Engl.* **1994**, *33*, 803.